

TECHNICAL RESEARCH REPORT

Recognizing Geometrically Complex Beams using Compliance
Metric in MEMS Extraction

by S. Bellam, S.K. Gupta, A. K. Priyadarshi

TR 2002-56



ISR develops, applies and teaches advanced methodologies of design and analysis to solve complex, hierarchical, heterogeneous and dynamic problems of engineering technology and systems for industry and government.

ISR is a permanent institute of the University of Maryland, within the Glenn L. Martin Institute of Technology/A. James Clark School of Engineering. It is a National Science Foundation Engineering Research Center.

Web site <http://www.isr.umd.edu>

Recognizing Geometrically Complex Beams using Compliance Metric in MEMS Extraction

S. Bellam, S.K. Gupta, A. K. Priyadarshi

Mechanical Engineering Department and Institute for Systems Research
University of Maryland
College Park, MD 20742

Abstract

This report describes a methodology to classify layout geometry as a beam structural element where geometric recognition fails due to shape complexity. FEA-based results are used to detect various structural elements in the layout. FEA-based simulation is applied to parts of the MEMS device layout to identify the relative stiffness of various elements in the layout. These stiffness maps provide valuable hints in correctly recognizing MEMS elements. For example, beam elements are relatively flexible when compared to the plate elements. We anticipate that such a methodology will make the extraction of structural elements for the device layout more robust.

1 Introduction

MicroElectro Mechanical Systems (MEMS) [Byrz94, Howe90, Tang97] are made up of extremely small mechanical elements, often integrated together with electronic circuitry. Micromachining, the enabling technology for MEMS device fabrication, is the technique for making structures and moving parts whose sizes are in the order of microns. These technologies are capable of making motors, pivots, linkages, and other mechanical devices of extremely small sizes. Micromechanical parts tend to be rugged, respond rapidly, use very little power, occupy very little space and have several other advantages over conventional macro machines. These devices have wide range of applications - inertial sensors, thermal sensors, optical switches etc.

A MEMS device is made up of various fundamental structural elements [Fedd99]. The set of these elements includes beams (long rectangular structural elements connected to other elements on its shorter edges), plates/masses (a structural element with more than two nearest neighbor elements, an anchor (an immobile structural element), a gap (usually between two beams; if the two beams are at different electrostatic potential then it is an electrostatic gap else it is a mechanical gap). Joints are abstract fundamental elements attached to the beams to describe the interconnections between the beams. These elements can be connected to form a MEMS component. Components can include springs and comb drives. Springs such as U-springs, serpentine springs and folded-flexure springs are compliant structures consisting of beams and joints commonly used in MEMS designs to control the movement of plate/mass. Comb structures such as the linear comb, differential comb are used to translate mechanical motion into electrical voltage (as an electromechanical sensor) or vice-versa (an electromechanical actuator) [Tang90]. Comb drives tend to consist of several regularly placed cantilever beams (fingers) separated by electrostatic gaps. MEMS components are themselves interconnected to form a MEMS device.

Bikram *et al.* developed a new MEMS design verification methodology using schematics extracted from device layouts [Baid98a, Baid98b]. VLSI designers have used such methodology extensively. Designers can perform fast simulation on reconstructed schematics thus reducing the time taken to verify a design layout. Bikram *et al.* devised simple geometric rules to recognize various structural elements in a MEMS layout. For example, a beam is defined as a rectangular element with its shorter sides bound. Such simple geometric rules fail to recognize geometrically complex beams.

This report describes a methodology to classify layout geometry as a beam structural element where geometric recognition fails due to shape complexity. FEA-based results are used to detect various structural elements in the layout. FEA-based simulation is applied to parts of the MEMS device layout to identify the relative stiffness of various elements in the layout. These stiffness maps provide valuable hints in correctly recognizing MEMS elements. For example, beam elements are relatively flexible when compared to the plate elements. Such a methodology would make the extraction of structural elements for the device layout more robust. The remainder of the report is organized as follows. Section 2 describes the background on beam theory. Section 3 describes the finite element method used to solve the FEA problem. Section 4 describes the method used to classify structural elements as beams using this methodology. Section 5 describes examples of beams that have been recognized using this methodology.

2 Beam Theory

Structural members are usually classified according to the types of loads they support. Structural members subjected to lateral forces, that is, forces or moments having their vectors perpendicular to the axis of the bar are called beams [Gere97, Timo35]. The beams shown in Figure 1 are classified as planar structures because they lie in a single plane. If all loads act in the same plane and if all deflections (shown by the dashed lines) occur in that plane, the plane is referred to as the “plane of bending”. Beams are usually described by the manner in which they are supported. Figure 1 shows a few types of beams. Figure 1(a) is a simply supported beam or a simple beam. The essential feature of this kind of a beam is the pin support at one end and a roller support at the other end. A pin support prevents translation but does not prevent rotation. A roller support prevents translation in a single direction. Figure 1(b) shows a cantilever beam. A cantilever beam is fixed at one end and free at the other. The fixed end cannot translate nor rotate. The free end can do both. Figure 1(c) shows a beam with an overhang. The overhanging portion is similar to the cantilever beam except that the beam axis may rotate at the support.

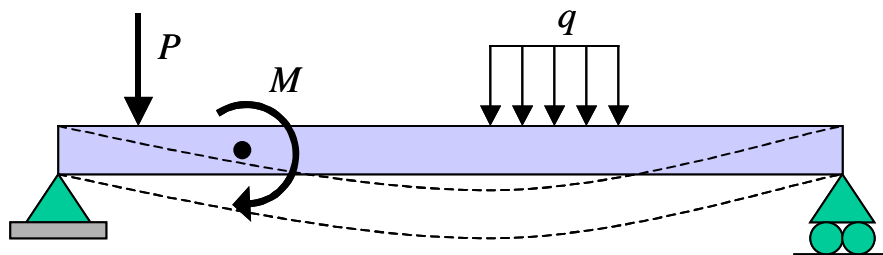


Figure 1(a): Simply Supported Beam

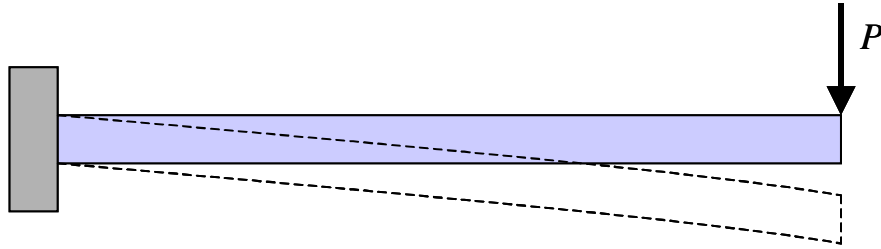


Figure 1(b): Cantilever Beam

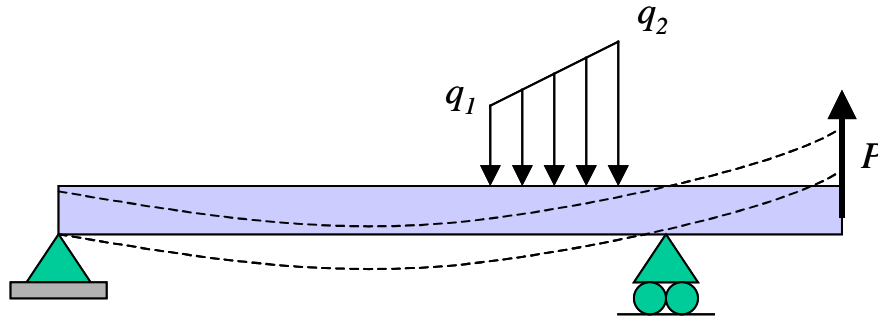


Figure 1(c): Beam with overhang

Several types of loads that can act on beams have been illustrated in Figure 1. When a load is applied over a very small area or a point, it can be idealized as a concentrated load such as the load P in Figures 1(a), (b) and (c), which is a single force. When the load is spread along the axis of the beam, it is represented as a distributed load. Distributed loads are measured by their intensity, which is expressed as force per unit length. Figure 1(a) shows a uniformly distributed load, which has a constant intensity q per unit distance. Figure 2(c) shows a linearly varying load with intensity varying linearly from q_1 to q_2 . Another kind of load is a couple, which is illustrated in Figure 1(a) with a moment M . In this report, we assume that the loads act in the plane of the figure; couples have their moment vectors perpendicular to the plane of the figure; and that the beam is symmetric with respect to the plane. This implies that every cross-section of the beam must have a vertical axis of symmetry, and the beam will deflect only in the “plane of bending”.

When forces or couples load a beam, the beam undergoes deflection and strains and stresses are created throughout the beam. To determine the deflection of the beam the internal forces and couples need to be calculated. Figure 2 shows an example of a cantilever beam loaded by a point force P . It illustrates a cross section of the beam cut at $m-m'$, which is located at a distance x from the free end, with shear force V and moment M acting on it to keep the cut beam in equilibrium. Using equations of equilibrium we can calculate the shear force and moment as:

$$V = P$$

$$M = Px$$

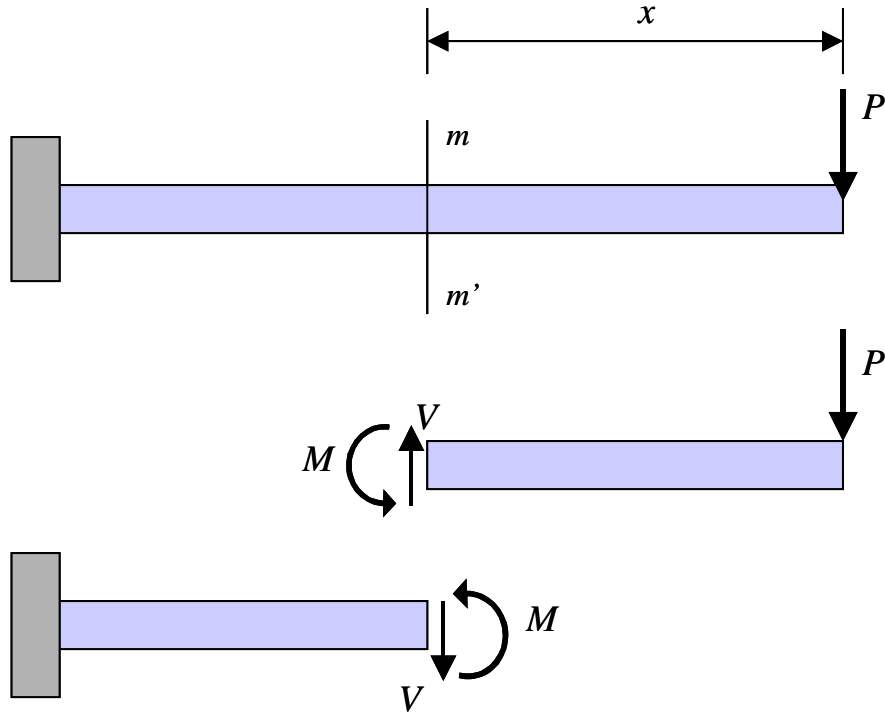


Figure 2: Shear force V and bending moment M in a beam

In a general case the shear force and moments are calculated using the relationships:

$$\frac{dV}{dx} = -q \quad (1)$$

$$V_B - V_A = -\int_A^B q dx \quad (2)$$

Equation 1 indicates that the rate of change of shear force is equal to the negative of the intensity of the distributed load at that point. Equation 2 indicates that the change in shear force between two points along the axis of a beam is equal to the negative of the total load between the two points. This is valid only for distributed loads. For point loads, an abrupt change in the shear force occurs at the point where the point load acts. Shear force does not change at the point of application of a couple [Timo35].

$$\frac{dM}{dx} = V \quad (3)$$

$$M_B - M_A = \int_A^B V dx \quad (4)$$

Equation 3 indicates that the rate of change of the bending moment is equal to the shear force at that point. This is true only for distributed loads and is not valid in regions where point loads act. Equation 4 indicates that the difference in bending moments between two points on a beam is equal to the integral of the shear force along the beam between the two points. This is also valid for point loads and is equal to the area below

the shear force diagram between the two points as shown in Figures 3 and 4. The bending moment at a point does not change when a point load acts at a point but the rate of change of bending moment changes abruptly. Equation 4 is not valid if a couple acts between the two points since the bending moment changes abruptly at the point of application of a couple.

Figure 3 shows a simple beam loaded with a point load and the resulting shear force diagrams and bending moment diagrams. It can be seen that the bending moment is the maximum at the point where the beam is loaded. Figure 4 shows a cantilever beam loaded with a point load at the free end. As can be seen from the shear force and bending moment diagrams, the bending moment is greatest at the fixed end and is non-existent at the free end and varies linearly between the two.

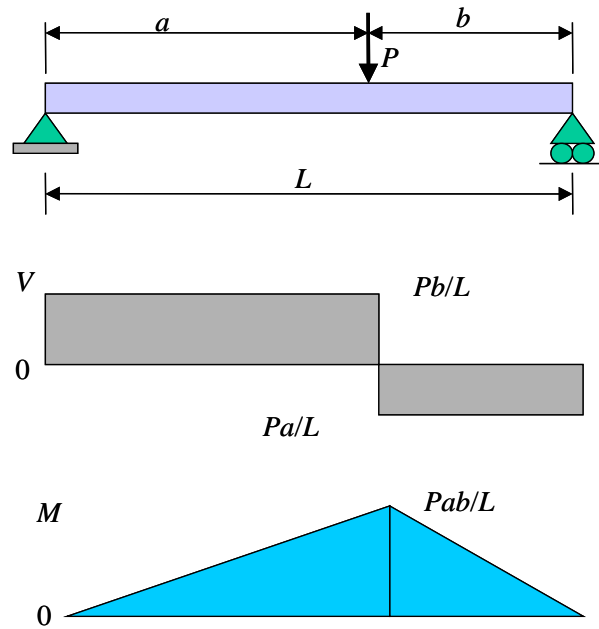


Figure 3: Shear-force and bending-moment diagrams for a simple beam and point load

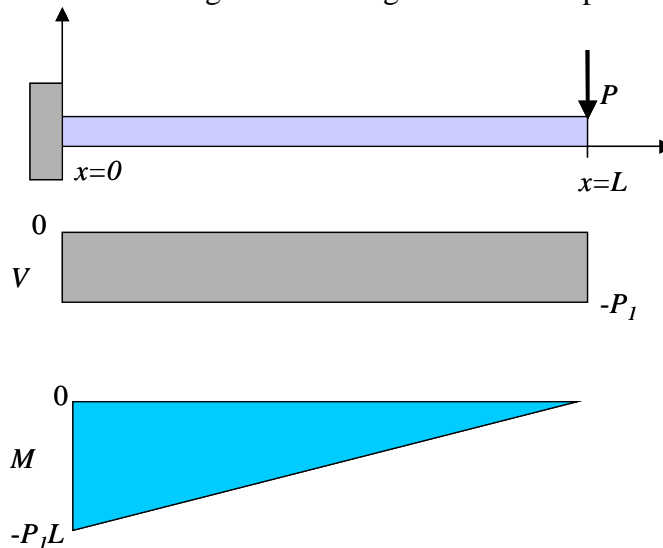


Figure 4: Shear-force and bending moment diagrams for a cantilever beam

The loads acting on the beam cause the beam to bend, thereby deforming the axis into a curve, known as the deflection curve. The deflection of the beam at any point along its axis is the displacement of that point from its original position. The deflection of the beam is directly related to the loads that act on the beam. The curvature of the deflection is a measure of how sharply a beam is bent at a point. We assume that the deflection of a beam is small compared to its length. Hence the radius of curvature can be defined as [Timo35] in Equation 5. Equation 6, known as the moment-curvature equation, shows that the curvature is directly proportional to the bending moment M and is inversely proportional to the quantity EI , where EI is known as the flexural rigidity of the beam.

$$\frac{1}{\rho} = \frac{d\theta}{dx} \quad (5)$$

$$\frac{1}{\rho} = \frac{M}{EI} \quad (6)$$

From equations 5 and 6, Equation 7 follows. In the case of the cantilever beam loading as shown in Figure 4, it is known that M is equal to a value $P(L-x)$ with the origin $x = 0$ at the fixed end. Hence Equation 7 can be rewritten in terms of the force and point of loading (Equation 8).

$$\frac{d\theta}{dx} = \frac{M}{EI} \quad (7)$$

$$\frac{d\theta}{dx} = \frac{P(L-x)}{EI} \quad (8)$$

Equation 8 shows that for a cantilever beam with a point force acting at a distance L from the fixed end the change in the angle of deflection in a beam between two close points is proportional to the relative distance of the point from the loading point and is inversely proportional to the moment of inertia at that point.

3 Finite Element Analysis

The fundamental concept of the finite element method is that any continuous quantity, such as temperature, pressure, or displacements, can be approximated by a discrete model composed of a set of piecewise continuous functions defined over finite number of sub-domains [Sege76]. The finite element method is a numerical procedure for solving disparate physical problems governed by a (partial) differential equation or the *energy theorem*. The finite element method can be divided into six basic steps [Stas85]. It is assumed that the problem is well posed, a global co-ordinate system is defined, and all pertinent geometric and material data are known.

1. *Discretization*. The structure or region being analyzed must be discretized into a suitable number of elements. Each element has several nodes associated with it depending upon the element type (8-node quad, triangular). Discretization results in the specification of the finite element mesh and involves defining the nodes and elements. Defining the elements involves defining the nodes associated with each element and its material properties. Nodal definitions are complete when the co-ordinates of each of the nodes are specified.

2. *Determination of the Local Element Characteristics.* Expressions for the local element characteristics, that is the element stiffness matrices and nodal force vectors must be derived from a suitable reference. If a local reference system is used, the reference changes from element to element. The element characteristics can be derived using either: (1) *variational method*; (2) *weighted residual methods* (e.g. collocation method, sub domain method, Galerkin method, and least square method) or (3) *potential energy formulation*. When using the Galerkin's method [Stas85], the weighting function for each unknown nodal value is defined and the weighted residual integral is evaluated. This generates one equation for each unknown nodal value. In the potential energy formulation, the potential energy of the system is written in terms of the nodal displacements and is then minimized. This gives one equation for each of the unknown displacements.

For structural problems, a plane stress or plane strain model can be followed to compute element characteristics. The first step is to compute the shape function matrix \mathbf{N} , which depends on the type of element. For an 8-node element \mathbf{N} is a 2×16 matrix, since each node has two degrees of freedom. The strain-nodal displacement matrix \mathbf{B} is calculated using Equation 9.

$$\mathbf{B} = \mathbf{L}\mathbf{N} \quad (9)$$

Where \mathbf{L} is linear operator matrix. \mathbf{L} is a 3×2 matrix. The material property matrix \mathbf{D} is computed using Equation 10 in the plane stress case and Equation 11 in the plane strain case. E is the Young's modulus and μ is the Poisson's ratio.

$$\mathbf{D} = \frac{E}{1-\mu^2} \begin{bmatrix} 1 & \mu & 0 \\ \mu & 1 & 0 \\ 0 & 0 & \frac{1-\mu}{2} \end{bmatrix} \quad (10)$$

$$\mathbf{D} = \frac{E}{(1+\mu)(1-2\mu)} \begin{bmatrix} 1-\mu & \mu & 0 \\ \mu & 1-\mu & 0 \\ 0 & 0 & \frac{1-2\mu}{2} \end{bmatrix} \quad (11)$$

The element stiffness matrix \mathbf{K}^e for a 2D problem is computed using Equation 12. Usually for 2D analysis, the problem structure or region is considered to have unit thickness or $t=1$. The element nodal force vectors \mathbf{f}^e is calculated by super position of the self-strain, pre-stresses, body forces, surface traction and point load force vectors. In simple problems where there are no self-stresses, pre-stresses and body forces, the elemental force vectors are calculated for only distributed and point loads. The force vectors for point loads can be calculated using Equation 13. \mathbf{f}_p is 2×1 matrix with magnitudes of the point loads in the x and y direction.

$$\mathbf{K}^e = \mathbf{B}^T \mathbf{D} \mathbf{B} \int_{A^e} t dx dy \quad (12)$$

$$\mathbf{f}_{PL}^e = \sum \mathbf{N}^T \mathbf{f}_p \quad (13)$$

The element characteristics \mathbf{K}^e and \mathbf{f}^e can describe the behavior of the element as seen in Equation 14. Vector \mathbf{d} is the unknown element nodal degrees of freedom

$$\mathbf{f}^e = \mathbf{K}^e \mathbf{d} \quad (14)$$

3. *Transformation of the Element Characteristics.* The element characteristics from Step 2 must be transformed from the local co-ordinate system to the global co-ordinate system. This is accomplished by using a transformation matrix. This step is required only when the local co-ordinate system is used in Step2.
4. *Assemblage of the Global Element Characteristics.* The individual element matrix representation of the equations generated in Step 2 can now be added together using a method of superposition (called as *direct stiffness method* in FEM) whose basis is nodal force equilibrium to obtain the global equations for the whole structure. The final assembled or global equation written in matrix form is given in Equation 15. Matrix \mathbf{a} is the nodal displacement matrix.

$$\mathbf{K}^a \mathbf{a} = \mathbf{f}^a \quad (15)$$

5. *Application of the Prescribed Displacements.* After the assemblage step, the assemblage stiffness matrix and the assemblage nodal force vector must be modified in order to impose the constraints on the restrained degrees of freedom. The matrix \mathbf{K}^a is singular unless the restraints on displacements are taken into account. The known displacement values in displacement matrix \mathbf{a} in Equation 15 are taken into account by modifying the elements in matrix \mathbf{K}^a and force vector \mathbf{f}^a are modified.
6. *Solution.* The elements in Equation 15 after modification are solved as a set of linear equations using one of the techniques such as: Gauss elimination technique, Gauss-Siedel iterative scheme, *SOR* (Successive Over Relaxation) schemes, conjugate gradient technique, *PCG* (Pre-conditioned Conjugate Gradient) techniques, etc. The nodal displacement matrix \mathbf{a} is calculated. Once the nodal displacement vectors are calculated, the nodal displacement can be post processed to calculate parameters such as strain and stress.

4 Compliance Hint Generation

In this section we describe a method, which can be used to determine if a set of atomic elements can be collectively classified as a beam. The 2D region that needs to be classified is set up as an FEA problem using a cantilever beam configuration and a point load. The point load used should be selected such that the deflection is not too large as Equation 8 is not valid for large deflections. If the point load is very small, the deflection may be too small to perform error-free computations. The method used to generate compliance hints is as follows:

1. Canonize [Baid98a] the portion of the layout, which cannot be recognized by geometric methods. The 2D region is represented by a set of rectangles, which are

canonized. If any of the resultant rectangles have an aspect ratio greater than 8, split the rectangle such that the resultant rectangles have a smaller aspect ratio. Re-canonize the layout.

2. Model each of the canonical rectangles in the resultant layout using a single 8-noded element such that vertices of the element and the rectangle coincide.
3. One of the shorter edges of the layout, which when extended does not intersect with the interior of the layout, is selected. The displacements of all nodes, which lie on the selected edge, are set to 0 in both directions. An edge parallel to the selected edge and at the maximum distance from it edge is now selected and the node closest to the center of the edge is selected. A point force is applied to it along the direction of the edge. The layout is assigned standard material properties. Figure 5 shows the placements of the nodes in an eight-nodded element and their co-ordinates.

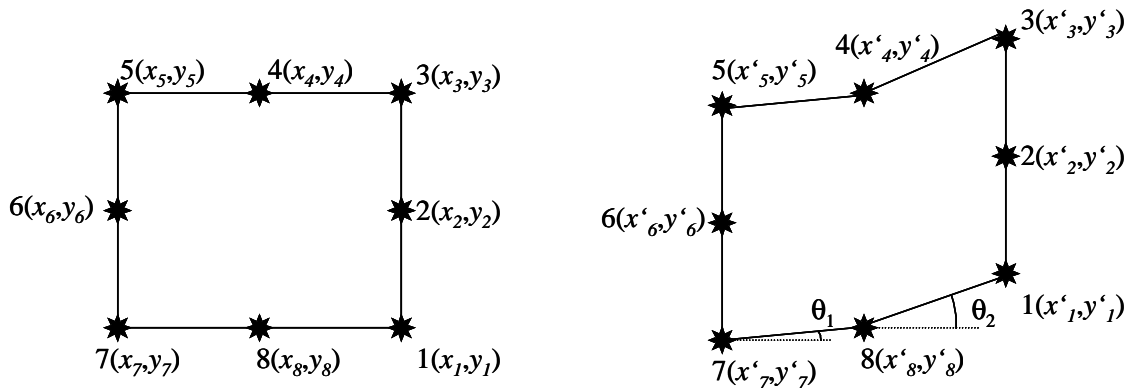


Figure 5. An 8-noded element before and after deflection

4. The FEA problem is solved using a standard FEA solver. The displacement of the individual nodes calculated by the solver for the applied boundary conditions and loads is recorded. The new nodal positions are calculated. Figure 5 shows the displaced nodes and their new co-ordinates.
5. The intensity of deflection an element, which is represented by Equation 5, is calculated at the point represented by node number 7, by approximating d/dx at that point to $z-1$ as shown in Figure 5. The result is normalized by dividing the result with a factor $(L-x)$, where L represents the horizontal distance between the boundary conditions and the applied load. x represents the horizontal distance between the point at which the intensity is being calculated and the boundary conditions. The result is called and is known as the *compliance metric*.
6. path connecting the boundary conditions and loading point is recognized such that it consists of abutting elements. is calculated for these elements. If the ratio of the 's for any two abutting elements is between 0.5 and 2, then the 2D region is classified as a beam.

5 Examples of Using Compliance Metric to Recognize Geometrically Complex Beams

In this section we describe examples where compliance metric is used to identify beam elements. The first example is that of a simple beam. The rectangle describing the 2D region is shown in Figure 6(a). Figure 6(b) graphically illustrates the FEA problem set up. The 2D region is *meshed* and the boundary conditions are specified. A point load P was applied as shown. The FEA problem is set up as a cantilever beam. The figure shows the numbered mesh elements. The compliance metric was computed for every element as specified in the previous section and the comparison chart is shown in Figure 6(c). As can be seen from the chart the compliance metric does not significantly vary from element to element. This result is in accordance with the beam properties as discussed in Section 2.




Figure 6(a): The 2D region described by the rectangle

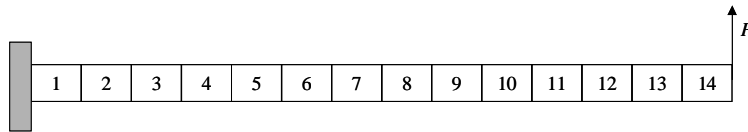


Figure 6(b): The FEA problem set up.

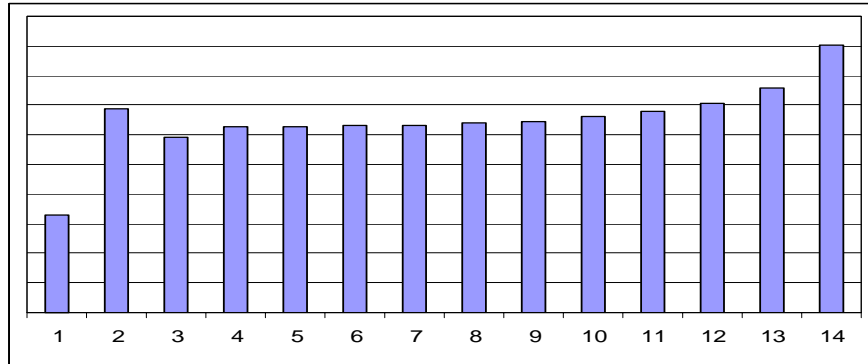


Figure 6(c): The compliance metric computed for the numbered elements in (b)

The 2D region as shown in Figure 7(a) was analyzed using the methodology described in Section 3. The region is a single large beam with two thin strips attached on either side. Figure 7(b) shows the extracted layout when purely geometric extraction rules are used. The 2D region is extracted as a set of two beams with mass elements in the middle. Figure 7(c) shows the meshed 2D region set up as cantilever beam problem for solving using FEA methods. Figure 7(d) shows the comparison of the compliance metric between each of the numbered elements. Figure 7(e) shows the extracted layout based on the methodology described in this report. The entire 2D region is extracted as a single beam.

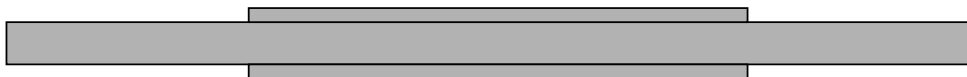


Figure 7(a): The 2D region being analyzed



Figure 7(b): Extracted layout based on purely geometric rules

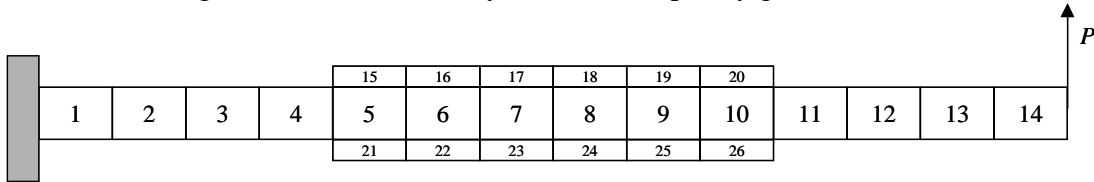


Figure 7(c): The FEA problem set up

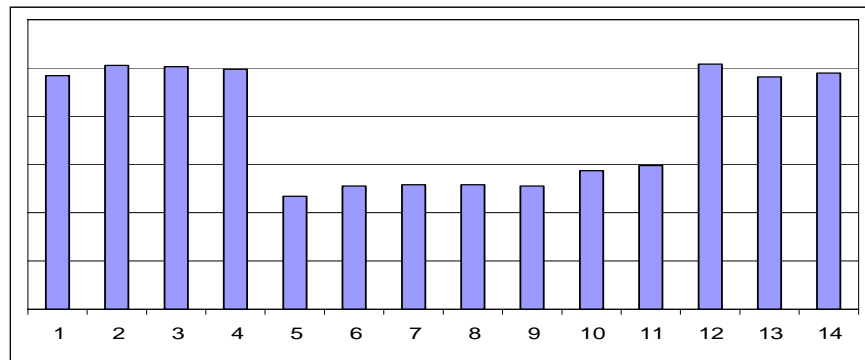


Figure 7(d): The compliance metric computed for the numbered elements in (c)



Figure 7(e): Extracted Layout based on compliance map

The 2D region as shown in Figure 8(a) was analyzed. The 2D region is a single large beam with two strips having considerable width attached on either side. Figure 8(b) shows the extracted layout when purely geometric extraction rules are used. The 2D region is extracted as a set of two beams with mass elements in the middle. Figure 8(c) shows the meshed 2D region set up as cantilever beam problem for solving using FEA methods. Figure 8(d) shows the comparison of the compliance metric between each of the numbered elements. As can be seen, the ratio of the compliance metric between neighboring elements varies by a large factor, hence the region cannot be classified as a single beam element. The extracted layout would be the same as the extracted layout based on geometric rules as seen in Figure 8 (b).

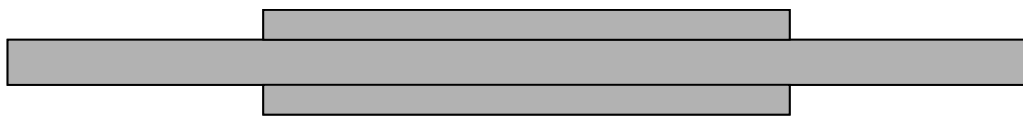


Figure 8(a): The 2D region being analyzed

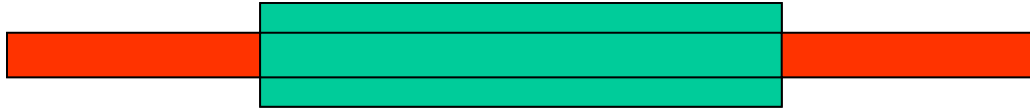


Figure 8(b): Extracted layout based on purely geometric rules

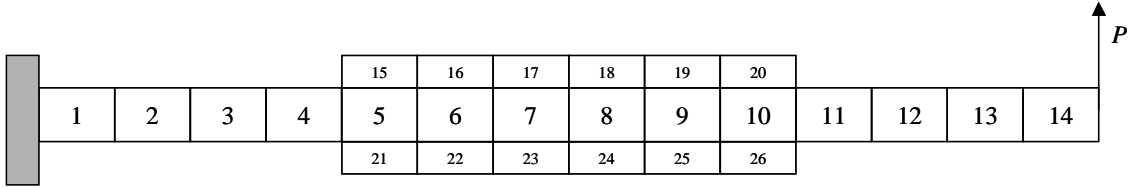


Figure 8(c): The FEA problem set up

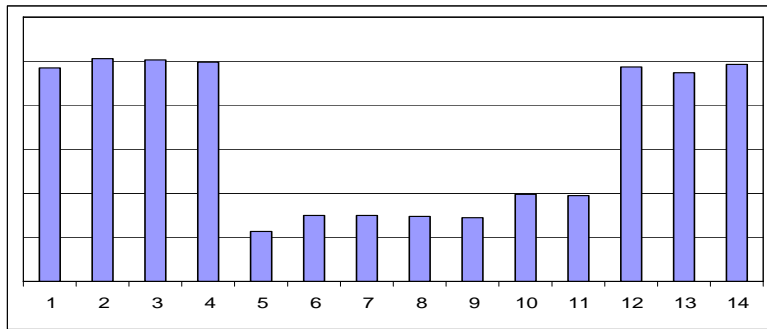


Figure 8(d): The compliance metric computed for the numbered elements in (c)

The 2D region as shown in Figure 9(a) was analyzed. The region is a single large beam with a section in the middle, which is slightly offset with respect to the rest of the beam. Figure 9(b) shows the extracted layout when purely geometric extraction rules are used. The 2D region is extracted as a set of three beams with joints in between. Figure 9(c) shows the meshed 2D region set up as a cantilever beam problem for solving using FEA methods. Figure 9(d) shows the comparison of the compliance metric between each of the numbered elements. Figure 9(e) shows the extracted layout based on the methodology described in this report. The entire 2D region is extracted as a single beam.



Figure 9(a): The 2D region being analyzed



Figure 9(b): Extracted layout based on purely geometric rules

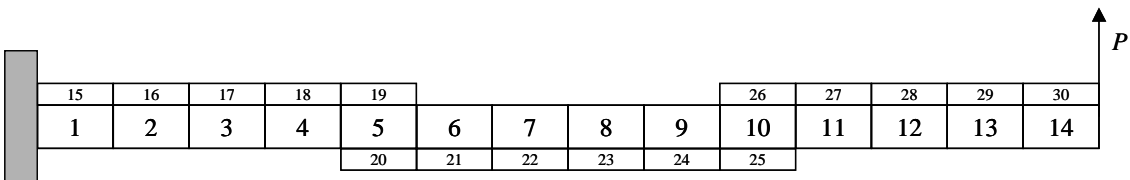


Figure 9(c): The FEA problem set up

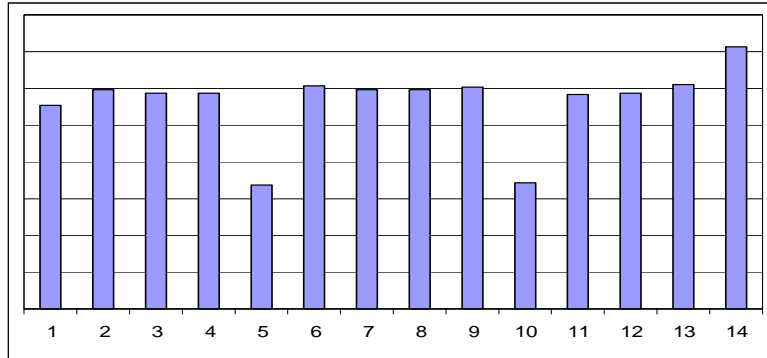


Figure 9(d): The compliance metric computed for the numbered elements in (c)



Figure 9(e): Extracted Layout based on compliance map

The 2D region as shown in Figure 10(a) was analyzed. The region is a single large beam with a section in the middle, which is offset by a considerable value with respect to the rest of the beam. Figure 10(b) shows the extracted layout when purely geometric extraction rules are used. The 2D region is extracted as a set of three beams with joints in between. Figure 10(c) shows the meshed 2D region set up as a cantilever beam problem for solving using FEA methods. Figure 10(d) shows the comparison of the compliance metric between each of the numbered elements. Since the compliance metric varies by a large amount the 2D region cannot be classified as a single beam.

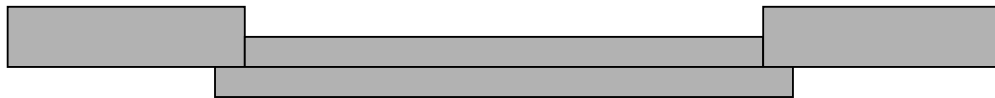


Figure 10(a): The 2D region being analyzed



Figure 10(b): Extracted layout based on purely geometric rules

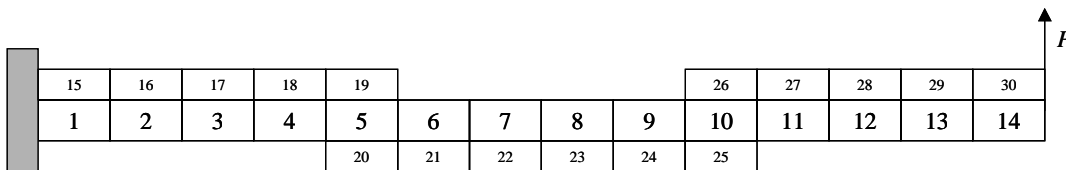


Figure 10(c): The FEA problem set up

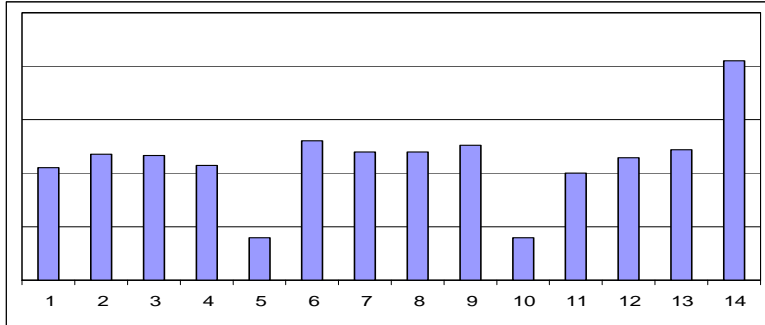


Figure 10(d): The compliance metric computed for the numbered elements in (c)

Acknowledgement. This research has been supported by a subcontract on NSF grant CCR9901171. Opinions expressed in this paper are those of authors and do not necessarily reflect opinions of the sponsors.

6 References

- [Baid98a] B. Baidya, S.K. Gupta and T. Mukherjee, "Feature-Recognition for MEMS Extraction," CDROM Proceedings of ASME Design Engineering Technical Conference, September 1998.
- [Baid98b] B. Baidya, S.K. Gupta and T. Mukherjee, "Device Extraction for Verification of MEMS"
- [Bryz94] J. Bryzek, K. Petersen and W. McCulley, "Micromachines on the march," *IEEE Spectrum*, May 1994, pp. 20-31.
- [Fed99] G. K. Fedder, "Structured Design of Integrated MEMS," *Proc. of MEMS '99*, Orlando, Florida, Jan.17-21, 1999, pp.1 -8.
- [Gere97] J.M. Gere and S.P. Timoshenko, *Mechanics of Materials*, PWS Publishing Company, 1997.
- [Howe90] R.T. Howe, *et. al.*, "Silicon Micromechanics," *IEEE Spectrum*, July 1990, pp. 29-35.
- [Sege76] L.J. Segerlind, *Applied Finite Element Analysis*, John Wiley and Sons, Inc, 1976.
- [Stas85] F.L. Stasa, *Applied Finite Element Analysis for Engineers*, CBS Publishing, 1985.
- [Tang90] W.C. Tang, T.-C.H. Nguyen, M.W. Judy and R. T. Howe, "Electrostatic-comb Drive of Lateral Poly-silicon Resonators," *Transducers '89*, Vol. 2, pp. 328-331, June 1990.

[Tang97] W.C. Tang, "Overview of Microelectromechanical Systems and Design Processes," *34th DAC Pro-ceedings*, 1997, pp. 670-3.

[Timo35] S. Timoshenko and G.H. MacCullough, *Elements of Strength of Materials*, D. Van Nostrand Company, Inc, New York, 1935.